A GEOMETRICAL POINT OF VIEW ON SINGULAR LINK FLOER HOMOLOGY

BENJAMIN AUDOUX

Abstract. We give a geometrical construction for singular link Floer homology $\widehat{\mathrm{HFV}}$, then we use it to prove that it vanishes for any singular connected sum of links.

Link Floer homology is an invariant of link in closed 3–manifolds which categorify the Alexander polynomial in the sense that the latter is recovered from the former as its graded Euler charasteristic. Alexander polynomial is one of the oldest known knot invariant. It leads to bounds for many geometrical properties of knot. Several of these bounds are turned into detection by the categorification. For instance, link Floer homology is known to detect Seifert genus, fiberedness, Thurston norm, *etc*.

On the other side, Alexander polynomial is known to be closely related to finite type invariant. Up to ambiant isotopy, a singular link is a smooth immersion of a finite number of circles in a 3–manifold such that the only singularities are a finite number of double points where two strands meet rigidly and transversely. There are three standard ways to desingularize a given double point. They are given in Fig. 1. Any algebraic invariant λ defined for regular links can be extended to singular links by stating recursively that the value of λ on a link with at least one double point p is the difference between its value on the positive desingularization of p and its value on the negative one. This can be encoded in the following formula:

$$\lambda(\times) = \lambda(\times) - \lambda(\times). \tag{1}$$

We say that λ is of finite type if there is an integer $k \in \mathbb{N}$ such that λ vanishes on every knot with at least k double points. Finite type invariant are conjectured to distinguish all knots. However, unlike link Floer homology, only few is known about how they can detect geometric properties of knots. Alexander polynomial coefficients are finite type invariants.

Hence, Alexander polynomial points, in one hand, to link Floer homology which have nice geometrical properties and, in the other hand, to finite type invariants, which are supposed to have such properties. It is tempting to use one to shed light on the other. At least, it is with this goal that I gave, in [Aud10], an extension $\widehat{\mathrm{HFV}}$ of link Floer homology for singular links in S^3 which categorify the relation (1). But sadly, the construction was combinatorial in nature and quite heavy to manipulate.

In this paper, we give a more geometrical construction of this extension which is closer to the original construction of Ozsvàth and Szabò. It is defined for oriented null-homologous singular link with oriented double points, in any $\mathbb{Z}$–sphere (and presumably in any closed 3–manifold), whereas the combinatorial

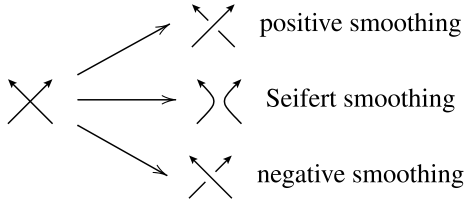

Figure 1: Desingularization of a double point: in a small planar neighborhood U of the double point, the three desingularizations correspond to the smoothing of the double point into, respectively, a positive crossing, no crossing or a negative crossing. The four diagrams are identical outside U.

version is only defined for such links in S^3. An orientation for a double point p of a link L is an orientation for the plane spanned by the vectors tangent to L at p. It is equivalent to the data of an order between the two strands.

Thanks to this geometrical approach, we prove the following proposition

Proposition. *Singular link Floer homology vanishes for every singular connected sum of links.*

which was only conjectured in [Aud10].

Finally, we give a conjecture about a finite type property possibly satisfied by link Floer homology.

1. Singular Heegaard diagrams

A singular Heegaard diagram is a quintuple $(\Sigma, \underline{\boldsymbol{\alpha}}, \underline{\boldsymbol{\beta}}, \underline{\boldsymbol{z}}, \underline{\boldsymbol{w}})$ where Σ is a closed surface of genus $g \in \mathbb{N}$, $\underline{\boldsymbol{\alpha}} = (\alpha_i), \underline{\boldsymbol{\beta}} = (\beta_i)$ are two sets of $(s + g + l - 1)$ disjoint circles on Σ, with $s, l \in \mathbb{N}^*$, and $\underline{\boldsymbol{z}} = (z_i), \underline{\boldsymbol{w}} = (w_i)$ sets of $2s + l$ distincts points on Σ such that:

i. $\underline{\boldsymbol{w}} \cap \underline{\boldsymbol{z}} = \emptyset$;
ii. circles from $\underline{\boldsymbol{\alpha}}$ and $\underline{\boldsymbol{\beta}}$ meet transversely;
iii. $\forall i \in [\![2s + 1, 2s + l]\!], w_i, z_i \notin \underline{\boldsymbol{\alpha}} \cup \underline{\boldsymbol{\beta}}$;
iv. $\forall i \in [\![1, s]\!], \{w_{2i}, w_{2i+1}, z_{2i}, z_{2i+1}\} \subset \beta_i$ and there is an arc in β_i joining w_{2i} to w_{2i+1} without meeting z_{2i} nor z_{2i+1};
v. every connected component of $\Sigma \setminus \underline{\boldsymbol{\alpha}}$ is a punctured sphere containing exactly one point from $\underline{\boldsymbol{w}}$ and one from $\underline{\boldsymbol{z}}$;
vii. every connected component of $\Sigma \setminus \bigcup_{i=s+1}^{s+\lambda} \beta_i$ is a punctured sphere containing exactly either one point w_i from $\underline{\boldsymbol{w}}$ and another point z_j from $\underline{\boldsymbol{z}}$ with $i, j \in [\![2s + 1, 2s + l]\!]$ or a circle $\beta_k \in \underline{\boldsymbol{\beta}}$ with $k \in [\![1, s]\!]$.

The elements of $\underline{\boldsymbol{\beta}}_s := \{\beta_i\}_{i\in[\![1,s]\!]} \subset \underline{\boldsymbol{\beta}}$, $\underline{\boldsymbol{z}}_s := \{z_i\}_{i\in[\![1,2s]\!]} \subset \underline{\boldsymbol{z}}$ and $\underline{\boldsymbol{w}}_s := \{w_i\}_{i\in[\![1,2s]\!]} \subset \underline{\boldsymbol{w}}$ are called *singular*. Other elements are called *regular* and we denote, respectively, by $\underline{\boldsymbol{\beta}}_r$, $\underline{\boldsymbol{z}}_r$ and $\underline{\boldsymbol{w}}_r$ the sets $\underline{\boldsymbol{\beta}} \setminus \underline{\boldsymbol{\beta}}_s$, $\underline{\boldsymbol{z}} \setminus \underline{\boldsymbol{z}}_s$ and $\underline{\boldsymbol{w}} \setminus \underline{\boldsymbol{w}}_s$.

Convention 1.1. Throughout this paper, the convention is to represent $\underline{\boldsymbol{\alpha}}$–objects with blue pictures, $\underline{\boldsymbol{\beta}}$–objects with red ones, $\underline{\boldsymbol{z}}$–points with black dots and $\underline{\boldsymbol{w}}$–points with white ones. I deeply apologize to the reader who has only a white and black access to this paper.

To any singular Heegaard diagram, one can associate a singular link in a 3–manifold Y as follows:

Prop. v. (resp. vi.) assures that the elements of $\underline{\boldsymbol{\alpha}}$ (resp. $\underline{\boldsymbol{\beta}}$) generate a g-dimensional subspace of $H_1(\Sigma; \mathbb{Z})$. Hence they specify an handlebody $H_{\underline{\alpha}}$ (resp. $H_{\underline{\beta}}$) bounded by Σ. The manifold Y is obtained by gluing $H_{\underline{\alpha}}$ and $H_{\underline{\beta}}$ along Σ. Then, on every connected component C of $\Sigma \setminus \underline{\boldsymbol{\alpha}}$ (resp. $\Sigma \setminus \underline{\boldsymbol{\beta}}_r$ such that $C \cap \underline{\boldsymbol{\beta}}_s = \emptyset$) we draw an embedded oriented arc joining the element of $\underline{\boldsymbol{z}}$ (resp. $\underline{\boldsymbol{w}}$) to the element of $\underline{\boldsymbol{w}}$ (resp. $\underline{\boldsymbol{z}}$) that C contains and then, we push this arc inside $H_{\underline{\alpha}}$ (resp. $H_{\underline{\beta}}$). Up to isotopy in $H_{\underline{\alpha}}$ (resp.$H_{\underline{\beta}}$), the arcs are uniquely defined since C is a punctured sphere and every puncture correspond to a disk in $H_{\underline{\alpha}}$ (resp.$H_{\underline{\beta}}$). Finally, for every singular circle β, we join the elements of $\underline{\boldsymbol{w}}$ to the elements of $\underline{\boldsymbol{z}}$ that β contains by two once-intersecting oriented arcs in a disk in $H_{\underline{\beta}}$ which is bounded by β. Up to isotopy, there is a unique way to do it. The union of all these arcs is an oriented singular link $L \subset Y$.

Remark 1.2. There is an obvious one-to-one correspondence between double points of L and the elements of $\underline{\boldsymbol{\beta}}_s$.

An alternative but equivalent description is to consider a self-indexed Morse–Smale function $f : M \longrightarrow \mathbb{R}$ and a gradient-like vector filed ξ for f such that $f^{-1}(3/2) \cong \Sigma$ and such that $\underline{\boldsymbol{\alpha}}$ (resp. $\underline{\boldsymbol{\beta}}$) correspond to the intersections of Σ with the flowlines of ξ starting at some index 1 critical point (resp. finishing at some index 2 critical point). Then the link corresponds to the union of the flowlines, with same orientation, passing through the points $\underline{\boldsymbol{z}}$ and the flowlines, with inversed orientation, passing through the points $\underline{\boldsymbol{w}}$.

Proposition 1.1. *Every oriented singular link L in a 3–manifold Y admits a singular Heegaard diagram presentation such that regular elements of $\underline{\boldsymbol{z}}$ (resp. $\underline{\boldsymbol{w}}$) are in bijection with regular components of L (components with no double point).*

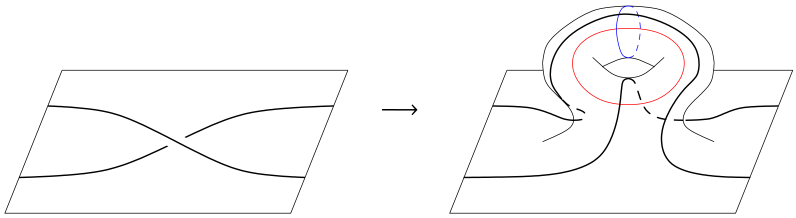

Figure 2: Uncrossing a crossing

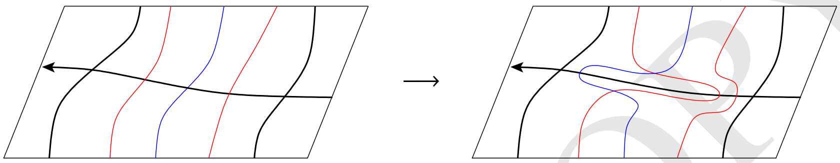

Figure 3: Localizing $L \cap (\underline{\boldsymbol{\alpha}} \cup \underline{\boldsymbol{\beta}})$ near the double points of L

Proof. First, we consider a self-indexed Morse-Smale function on Y and a gradient-like vector field ξ for f. We denote by $(\Sigma, \underline{\boldsymbol{\alpha}}, \underline{\boldsymbol{\beta}})$ the associated Heegaard diagram.

Then, we consider a representative for L which is in general position with regard to ξ. It means that

i. L avoids the closure of the (finitely many) flowlines of ξ which connect two critical points with consecutive indices;
ii. every flowline of ξ meets L at most twice, and the intersections are always transverse;
iii. only a finite number of flowlines of ξ meet L exactly twice;
iv. there are a finite number of intersections betwen L and the stable (resp. unstable) manifolds associated to the critical points of index 1 (resp. 2).

Now, we can push L along ξ to Σ. It leads to a diagram on Σ with a finite number of crossings. Every crossing can be be "uncrossed" by stabilizing Σ as shown in Fig. 2. At this stage, L is embedded on Σ. It may cross the $\underline{\boldsymbol{\alpha}}$ and $\underline{\boldsymbol{\beta}}$–circles in a finite number of non-singular points. Now we choose arbitrarily an origin on every regular component of L. By performing some finger moves, shown in Fig. 3, on the elements of $\underline{\boldsymbol{\alpha}} \cup \underline{\boldsymbol{\beta}}$, we may assume that every such crossing is in a neigborhood of either a double point of L or the origin of a regular component. Moreover, we may assume that the intersections with $\underline{\boldsymbol{\alpha}}$ are just before the double point or the origin point, with respect to the orientation of L, and the intersections with $\underline{\boldsymbol{\beta}}$ just after. We complete $\underline{\boldsymbol{\alpha}}$ and $\underline{\boldsymbol{\beta}}$ by adding two elements in each for every double point and every regular component, and we set $\underline{\boldsymbol{z}}$ and $\underline{\boldsymbol{w}}$ as shown in Fig. 4. Finally, we remove one of the added $\underline{\boldsymbol{\alpha}}$–circles and one of the regular $\underline{\boldsymbol{\beta}}$–ones. □

Remark 1.3. For oriented singular knots K in S^3, a singular Heegaard diagram presentation can be directly associated to any connected planar diagram D with one distinguished point. To this end, we consider D_s, obtained from D by making singular all its crossing. The surface Σ is the border of a thickening H_s of D_s in $\mathbb{R}^3$. The family $\underline{\boldsymbol{\alpha}}$ is partially defined as the border of every bounded regions in $\mathbb{R}^2 \setminus (H_s \cap \mathbb{R}^2)$. The thickening of the distinguished point of D leads to a disk whose border, denoted by β_0, belongs to $\underline{\boldsymbol{\beta}}$. For $\underline{\boldsymbol{z}}$ and $\underline{\boldsymbol{w}}$, we yet choose two points z and w on Σ such that they are on both sides of β_0 and such that an arc from z to w inside H_s meets the disk borded by β_0 with the same intersection number than D_s. Finally, we complete $\underline{\boldsymbol{\alpha}}$, $\underline{\boldsymbol{\beta}}$, $\underline{\boldsymbol{z}}$ and $\underline{\boldsymbol{w}}$ by adding, for every crossing of D, the elements given in Fig. 5.

Theorem 1.2. *Two singular Heegaard diagrams describe the same singular link iff they can be connected with a finite sequence of:*

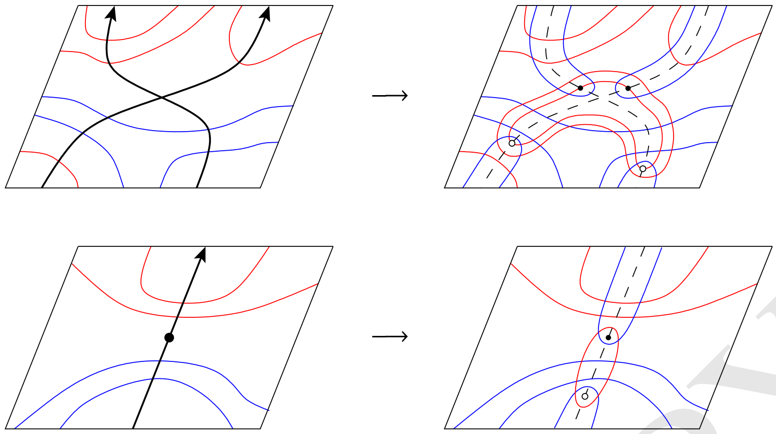

Figure 4: Addition of circles and definition of $\underline{\boldsymbol{z}}$ and $\underline{\boldsymbol{w}}$

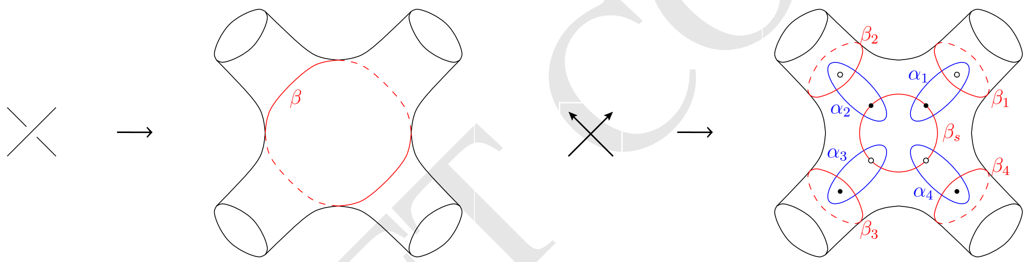

Figure 5: Singular Heegaard diagrams around planar crossing

$\boldsymbol{\alpha}$–isotopies: *isotopy of an element $\alpha \in \underline{\boldsymbol{\alpha}}$ in the complement of $\underline{\boldsymbol{z}}$, $\underline{\boldsymbol{w}}$ and $\underline{\boldsymbol{\alpha}} \setminus \alpha$;*
$\boldsymbol{\beta}$–isotopies: *isotopy of an element $\beta \in \underline{\boldsymbol{\beta}}$ in the complement of $\underline{\boldsymbol{z}}$, $\underline{\boldsymbol{w}}$ and $\underline{\boldsymbol{\beta}} \setminus \beta$;*
$\boldsymbol{\alpha}$–handleslides: *handleslide in the complement of $\Sigma \setminus \underline{\boldsymbol{\alpha}}$ between two elements of $\underline{\boldsymbol{\alpha}}$ (see Fig. 6);*
regular $\boldsymbol{\beta}$–handleslides: *handleslide in the complement of $\Sigma \setminus \underline{\boldsymbol{\beta}}$ between two elements of $\underline{\boldsymbol{\beta}}_r$ (see Fig. 6);*
singular $\boldsymbol{\beta}$–handleslides: *handleslide in the complement of $\Sigma \setminus \underline{\boldsymbol{\beta}}$ of $\beta \in \underline{\boldsymbol{\beta}}_s$ over $\beta' \in \underline{\boldsymbol{\beta}}_r$ (see Fig. 6);*
index zero/three (de)stabilizations: *adding (resp. removing) one element in $\underline{\boldsymbol{\alpha}}$, $\underline{\boldsymbol{\beta}}_r$, $\underline{\boldsymbol{z}}$ and $\underline{\boldsymbol{w}}$ as in Fig. 7(a);*
index one/two (de)stabilizations: *increasing (resp. reducing) the genus of Σ by one and adding (resp. removing) one element in $\underline{\boldsymbol{\alpha}}$ and $\underline{\boldsymbol{\beta}}_r$ as in Fig. 7(b).*

Remark 1.4. **This statement is very likely** to be refined into an admissible version. It would lead, *ipso facto*, to a definition of $\widehat{\mathrm{HFV}}$ for singular links in any closed 3–manifold.

Proof. Let $D = (\Sigma, \underline{\boldsymbol{\alpha}}, \underline{\boldsymbol{\beta}}, \underline{\boldsymbol{z}}, \underline{\boldsymbol{w}})$ be a singular Heegaard diagram.

First we localize the singularities of D in a finite number of blisters. Actually, every singular circle $\beta \in \underline{\boldsymbol{\beta}}_s$ is contained in a punctured sphere whose border is a union of regular circle from $\underline{\boldsymbol{\beta}}_r$. Hence, up to singular $\boldsymbol{\beta}$–handleslides, we can assume that any singular circle β bounds a disk in $\Sigma \setminus \underline{\boldsymbol{\beta}}$ and, up to regular $\boldsymbol{\beta}$–handleslides, that β is parallel in $\Sigma \setminus \underline{\boldsymbol{\beta}}$ to a circle from $\underline{\boldsymbol{\beta}}_r$ (see Fig. 8). If $\Sigma \setminus \underline{\boldsymbol{\beta}}_r$ is connected, we perform first a zero/three–stabilization in order to get a reguler $\boldsymbol{\beta}$–circle we can slide over the other $\boldsymbol{\beta}$–circles.

Then, since singular circles behave as points through which regular $\underline{\boldsymbol{\beta}}$–circles can be moved thanks to regular $\boldsymbol{\beta}$–handleslides over the surrounding regular circles, it follows from standard Morse theory that any isotopy which fixes a neighborhood of the double points can be obtained using the elementary regular moves.

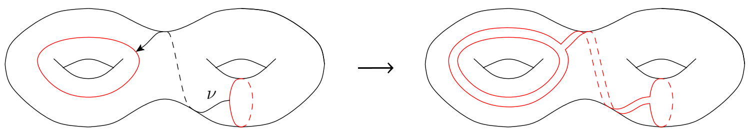

Figure 6: Handleslide: for every arc ν between two cirles c_1 and c_2, the handleslide of c_1 over c_2 is the replacement of c_1 by the connected sum of c_1, a parallel copy of c_2 and the border of a thickening of ν. If c_1 is singular, then the result depend on where ν points on it.

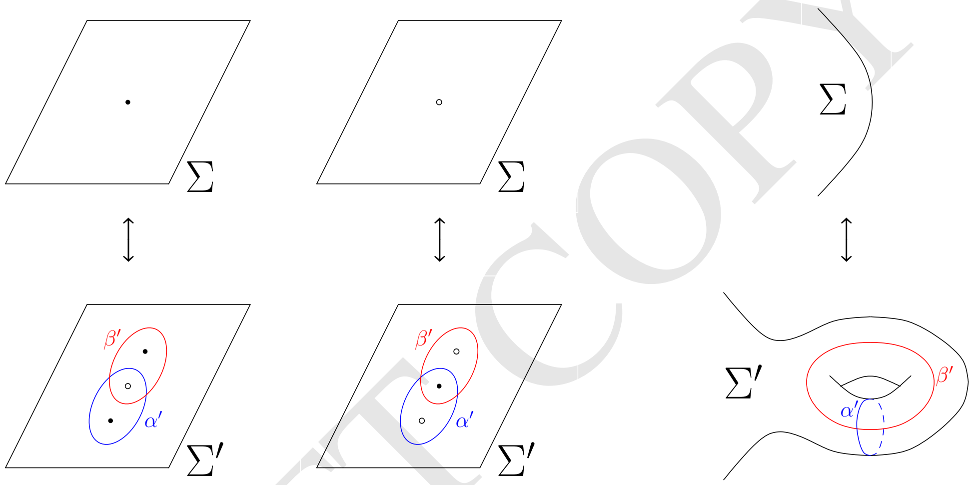

(a) zero/three (de)stabilization (z, z_1', w and w_1' may be singular)

(b) one/two (de)stabilization

Figure 7: Stabilizations

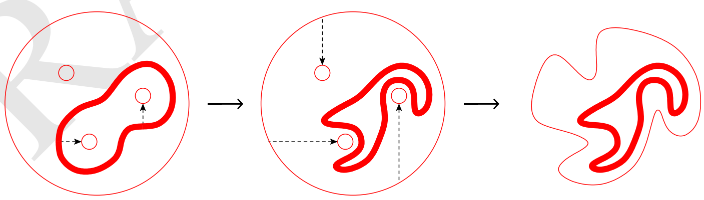

Figure 8: Localizing singular circles: Thin circles are regular β–circles whereas the fat one is a singular circle. Dotted arcs represent the handleslides.

However, to obtain all isotopies, we may need to flip the double points. This can done using singular $\boldsymbol{\beta}$–handleslides (see Fig. 9). □

Now we assume that Σ is oriented by the out orientation of H_β. Then singular Heegaard diagrams are convenient for dealing with both positive and negative desingularization of any double point of associated singular links.

Proposition 1.3. *Let L be a singular link and D a singular Heegaard diagram for it. Let p be a double point of L and β_p the singular arc in D corresponding to it. Then, D_+ and D_-, obtained by slightly deforming β_p*

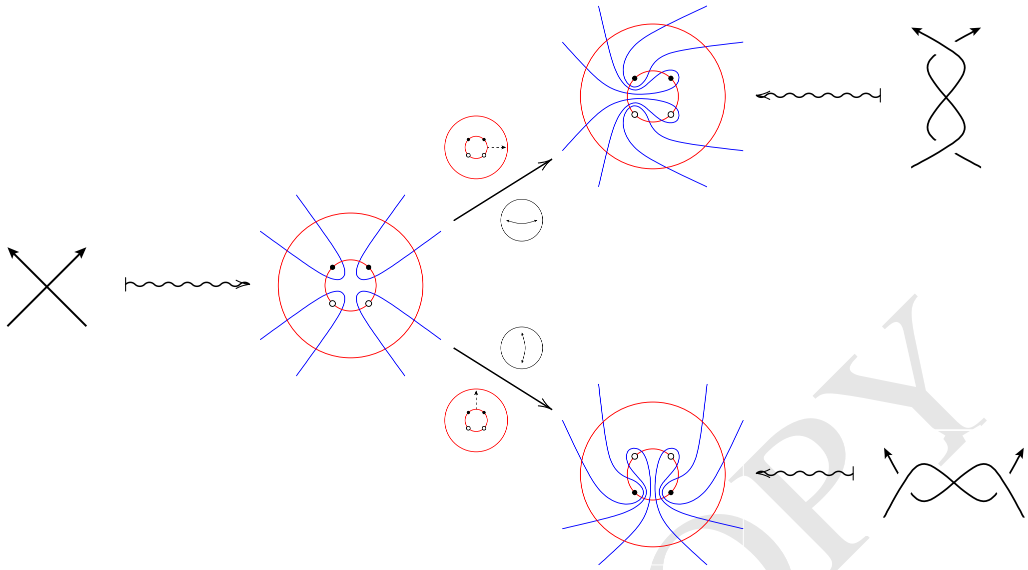

Figure 9: Flipping double points

in D as follows:

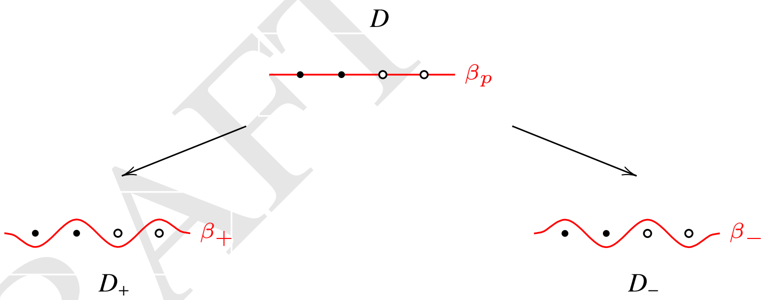

,

are Heegaard diagrams for, respectively, the positive and the negative resolution of p.

Proof. According to point vii. of the definition of singular Heegaard diagrams, the arc β_p splits a connected component of $\Sigma\backslash\underline{\beta}_r$ in two parts which are not containing any element of $\underline{z}$ nor of $\underline{w}$. Thus distributing the two elements of $\underline{z}$ and the two elements of $\underline{w}$ which are on β_p to these two connected components of $\Sigma \setminus (\underline{\beta}_r \cup \beta)$ leads to a new Heegaard diagram with one singular arc less.

Then Fig. 10 shows how the two considered deformations of β_p act on the associated singular link in a neighbourhood of a disk borded by β_p in $H_{\underline{\beta}}$. □

2. Singular link Floer homology

2.1. **A quick review of link Floer homology.** In this part, we review some definitions and propositions from usual link Floer homology theory. For complete proofs and thorought treatments, we refer the reader to [OS04c], [OS04b], [OS06a], [OS04a], [Ras03], [OS08] and [OS05]; for more introductory papers, we refer to [OS06b],[OS06c]; and for an intermediate discussion, to [Sah10].

Let Σ be a closed oriented surface, l a positive integer, $(\underline{\alpha}^i)_{i\in\mathbb{N}}$ a sequence of families of l disjoint circles on Σ such that, for any distincts indices i and j, $\underline{\alpha}^i$ and $\underline{\alpha}^j$ intersects transversely, and $\underline{z}$ a multipoint on $\Sigma \setminus (\bigcup_{i\in\mathbb{N}} \underline{\alpha}^i)$ such that, for every $i \in \mathbb{N}$, $\underline{z}$ meets at least once every connected component of $\Sigma \setminus \underline{\alpha}^i$.

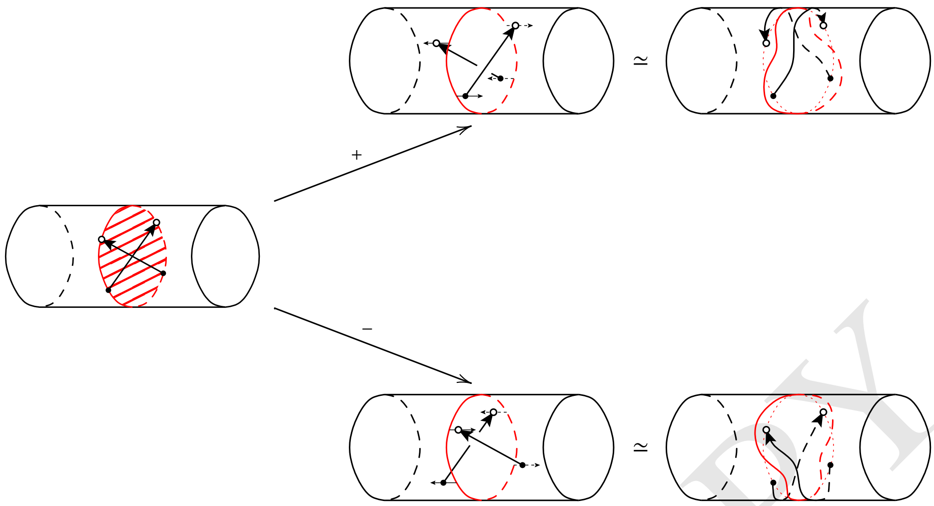

Figure 10: Desingularizations of a singular circle

We define $\mathrm{Sym}^l(\Sigma)$ as the symetrized product of l copies of Σ, *i.e.* $\Sigma^l/_{\mathfrak{S}_l}$ where $\mathfrak{S}_l$ acts on Σ^l by permuting the coordinates. For every $i \in \mathbb{N}$, we denote by $\mathbb{T}_{\underline{\alpha}^i}$ the torus $\prod\limits_{\alpha\in\underline{\alpha}^i} \alpha$ seen as embedded in $\mathrm{Sym}^l(\Sigma)$. Because of the transversality condition, the tori $\mathbb{T}_{\underline{\alpha}^{i_1}}$ and $\mathbb{T}_{\underline{\alpha}^{i_2}}$, for distincts indices i_1 and i_2, meet in a finite number of points. We define $\widehat{\mathrm{CF}}(\underline{\alpha}^{i_1}, \underline{\alpha}^{i_2})$ as the module freely generated over $\mathbb{F}_2 := \mathbb{Z}/_{2\mathbb{Z}}$ by $\mathbb{T}_{\underline{\alpha}^{i_1}} \cap \mathbb{T}_{\underline{\alpha}^{i_2}}$.

Now, let $S = (\underline{\alpha}^{i_k})_{k\in[\![1,d]\!]}$ be a length $d \geq 2$ sequence of distincts elements of $(\underline{\alpha}^i)_{i\in\mathbb{N}}$. We define $f_S^{\underline{z}}\colon \bigotimes\limits_{k=1}^{d-1} \widehat{\mathrm{CF}}(\underline{\alpha}^{i_k}, \underline{\alpha}^{i_{k+1}}) \longrightarrow \widehat{\mathrm{CF}}(\underline{\alpha}^{i_1}, \underline{\alpha}^{i_d})$ as the linear map defined on every generator $\underline{\boldsymbol{x}} = \underline{\boldsymbol{x}}_1 \otimes \cdots \otimes \underline{\boldsymbol{x}}_{d-1}$, where $\underline{\boldsymbol{x}}_k \in \mathbb{T}_{\underline{\alpha}^{i_k}} \cap \mathbb{T}_{\underline{\alpha}^{i_{k+1}}}$ for all $k \in [\![1, d-1]\!]$, by

$$f_S^{\underline{z}}(\underline{\boldsymbol{x}}) = \sum_{\underline{\boldsymbol{y}}\in\mathbb{T}_{\underline{\alpha}^{i_1}}\cap\mathbb{T}_{\underline{\alpha}^{i_d}}} \left(\sum_{\substack{\phi\in\pi_2(\underline{\boldsymbol{x}}_1,\cdots,\underline{\boldsymbol{x}}_{d-1},\underline{\boldsymbol{y}})\\ \mu(\phi)=3-d\\ n_{\underline{z}}(\phi)=0}} \#\mathcal{M}(\phi).\underline{\boldsymbol{y}} \right),$$

where

- $\pi_2(\underline{\boldsymbol{x}}_1, \cdots, \underline{\boldsymbol{x}}_{d-1}, \underline{\boldsymbol{y}})$ is the set of homotopy classes of Whitney disks, *i.e.* of maps from the unit disk $\mathbb{D}$ to $\mathrm{Sym}^l(\Sigma)$ whose restriction to the boundary satisfy the conditions given in Fig. 11;
- an almost complex structure being given on $\mathrm{Sym}^l(\Sigma)$, $\mathcal{M}(\phi)$ is, up to reparametrizations of $\mathbb{D}$, the module space of representatives of ϕ which are pseudo-holomorphic;
- $\mu(\phi)$ is the Maslov index of $\mathcal{M}(\phi)$;
- since $\mathcal{M}(\phi)$ is, under the required condition, a finite set, $\#\mathcal{M}(\phi)$ denotes its cardinal modulo 2;
- $n_A(\phi)$ is the sum of geometric intersection numbers between ϕ and $\{z\} \times \mathrm{Sym}^{l-1}(\Sigma) \subset \mathrm{Sym}^l(\Sigma)$ for every element z of A.

The following property is essentially a consequence of the Gromov's compactness theorem from the eponym pseudoholomorphic curves theory:

Theorem 2.1 (Ozsvàth, Szabò). *For every positive integer s,*

$$\sum_{0\leq k<m\leq s} f^{\underline{z}}_{\underline{\alpha}^0,\cdots,\underline{\alpha}^k,\underline{\alpha}^m,\cdots,\underline{\alpha}^s} \circ (\mathrm{Id}^{\otimes k} \otimes f^{\underline{z}}_{\underline{\alpha}^k,\cdots,\underline{\alpha}^m} \otimes \mathrm{Id}^{\otimes(s-m)}) = 0.$$

Remark 2.1. For simplicity and since it is sufficient for our purpose, we deals with only the hat $\mathbb{F}_2$–version in this paper. However, the construction can be lifted to $\mathbb{Z}$–coefficients and a minus version can also be defined.

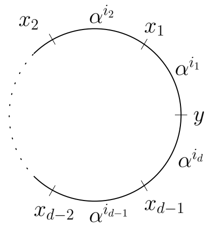

Figure 11: Model for Whitney disks: up to homotopy, a map $\phi\colon \mathbb{D} \longrightarrow \mathrm{Sym}^l(\Sigma)$ is a Whitney disk of $\pi_2(\underline{\boldsymbol{x}}_1, \cdots, \underline{\boldsymbol{x}}_{d-1}, \underline{\boldsymbol{y}})$ iff $\phi(1) = \underline{\boldsymbol{y}}$, $\phi\big(\{e^{-i\frac{2t\pi}{d}} \,|\, t \in [0,1]\}\big) \subset \underline{\boldsymbol{\alpha}}^{i_d}$ and, for every $k \in [\![1, d-1]\!]$, $\phi(e^{i\frac{2k\pi}{d}}) = \underline{\boldsymbol{x}}_k$ and $\phi(\{e^{i\frac{2t\pi}{d}} | t \in [k-1,k]\}) \subset \underline{\boldsymbol{\alpha}}^{i_k}$.

2.2. **A few definitions and notation for flags.** In this short part, we set notation for the following sections.

A flag is an increasing finite sequence of finite sets such that two successives differ only by one element. If the first element is A, we say that it starts at A. If the last element is B, we say it finishes at B. Then, we also say that it is joining A to B.

A flag will always be denoted by $\mathcal{F}^* := (F_1^* \subsetneq F_2^* \subsetneq \cdots \subsetneq F_{d^*}^*)$ where $*$ is either an element of $\mathbb{N}^*$ or void. The number d^* is called the *length* of $\mathcal{F}^*$.

For any two subsets A and B, we denote by $\mathscr{F}_A^B$ the set of flags which join A to B, by $\mathscr{F}_A^{\subset B}$ the set of those which join A to a subset of B and by $\mathscr{F}^{\subset B}$ the set of flags whose elements are all contained in B.

It will not make sense before the next section, but for any flag $\mathcal{F}$ and any pair of integer $1 \leq i < j \leq d$, we denote by $\boldsymbol{B}_{i,j}^{\mathcal{F}}$ the sequence $\underline{\boldsymbol{\beta}}_{F_i}, \underline{\boldsymbol{\beta}}_{F_{i+1}}, \cdots, \underline{\boldsymbol{\beta}}_{F_j}$ and by $\boldsymbol{\Theta}_{i,j}^{\mathcal{F}}$ the element $\underline{\boldsymbol{\theta}}_{F_i}^{F_{i+1}} \otimes \underline{\boldsymbol{\theta}}_{F_{i+1}}^{F_{i+2}} \otimes \cdots \otimes \underline{\boldsymbol{\theta}}_{F_{j-1}}^{F_j}$. Ommiting the indices i and j means that $i = 1$ and $j = d$. If $d = 1$, *i.e.* if $\mathcal{F}$ is reduced to a single finite set, then $\boldsymbol{B}^{\mathcal{F}}$ and $\boldsymbol{\Theta}^{\mathcal{F}}$ are just void.

2.3. **Singular link Floer homology.** Let L be a singular oriented link in a 3–manifold Y. We fix

- a Heegaard diagram $D = (\Sigma, \underline{\boldsymbol{\alpha}}, \underline{\boldsymbol{\beta}}, \underline{\boldsymbol{z}}, \underline{\boldsymbol{w}})$ for L;
- an orientation o for the $k \in \mathbb{N}$ double points of L.

2.3.1. *Chain complex.* Every double point p of L corresponds to a singular circle $\beta_p \in \underline{\boldsymbol{\beta}}_s$. The orientation $o_{|p}$ of p is an orientation for the disk bordered by β_p. It induces hence an orientation for β_p. Now we label the two elements of $\beta_p \cap \underline{\boldsymbol{z}}$ (resp. $\beta_p \cap \underline{\boldsymbol{w}}$) by z and z' (resp. w and w') in such a way that an oriented arc embedded in β_p and joining z' to z (resp. w' to w) without meeting $\underline{\boldsymbol{w}}$ (resp. $\underline{\boldsymbol{z}}$) has the same orientation as β_p. Now, we call the arc connecting z to w' without meeting w the *special arc* of β_p (see Fig. 13(b)).

According to Prop. 1.3, β_p gives rise to circles β_+ and β_-, avoiding the elements of $(\underline{\boldsymbol{z}} \cup \underline{\boldsymbol{w}}) \cap \beta_p$ and corresponding, respectively, to the positive and the negative desingularization of p. Note that here, we make a choice to determine in which connected component of $\Sigma \setminus \underline{\boldsymbol{\alpha}}$ the four elements of $\beta_+ \cap \beta_-$ lie.

For every $\beta \in \underline{\boldsymbol{\beta}}$, we choose a marked point $m_\beta \in \beta \setminus \underline{\boldsymbol{\alpha}}$. If $\beta \in \underline{\boldsymbol{\beta}}_s$, we require that m_β belongs to the special arc of β.

For every $A \subset \underline{\boldsymbol{\beta}}_s$ and to any $\beta \in \underline{\boldsymbol{\beta}}$, we associate β_A which is a circle isotopic to β_η in $\Sigma \setminus \underline{\boldsymbol{z}} \cup \underline{\boldsymbol{w}}$, where $\eta = -$ if $\beta \in A$, $\eta = +$ if $\beta \in \underline{\boldsymbol{\beta}}_s \setminus A$ and η is void if $\beta \notin \underline{\boldsymbol{\beta}}_s$. More specifically, we choose these circles as described in Fig. 12. We denote by $\underline{\boldsymbol{\beta}}_A$ the set $\{\beta_A\}_{\beta \in \underline{\boldsymbol{\beta}}}$ and we define $\widehat{\mathrm{CF}}(D)$ as the direct sum $\bigoplus\limits_{A \subset \underline{\boldsymbol{\beta}}_s} \widehat{\mathrm{CF}}(\underline{\boldsymbol{\alpha}}, \underline{\boldsymbol{\beta}}_A)$.

Now we consider $A \subset B \subset \underline{\boldsymbol{\beta}}_s$. If $A \neq B$, we denote by $\underline{\boldsymbol{\theta}}_A^B$ the generator of $\widehat{\mathrm{CF}}(\underline{\boldsymbol{\beta}}_A, \underline{\boldsymbol{\beta}}_B)$ described in Fig. 13. Then we can set

$$f_A^B\colon \begin{array}{ccc} \widehat{\mathrm{CF}}(\underline{\boldsymbol{\alpha}}, \underline{\boldsymbol{\beta}}_A) & \longrightarrow & \widehat{\mathrm{CF}}(\underline{\boldsymbol{\alpha}}, \underline{\boldsymbol{\beta}}_B) \\ \underline{\boldsymbol{x}} & \longmapsto & \displaystyle\sum_{\mathcal{F} \in \mathscr{F}_A^B} f_{\underline{\boldsymbol{\alpha}}, \boldsymbol{B}^{\mathcal{F}}}^{\underline{\boldsymbol{z}} \cup \underline{\boldsymbol{w}}}(\underline{\boldsymbol{x}} \otimes \boldsymbol{\Theta}^{\mathcal{F}}) \end{array},$$

where the notation is defined in sections 2.1 and 2.2.

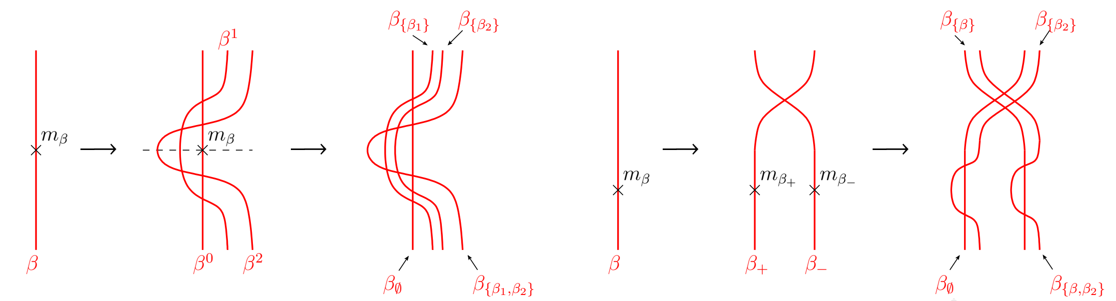

(a) If $\beta \in \underline{\beta}_r$, then we first rename β for β^0. Then, for $k \in [\![1, |\underline{\alpha}_s|]\!]$, we define successively β^k as a parallel copy of β on which we have performed a finger move along a line which is transverse to β in p_β and such that β^k meets exactly twice β^l for every $l \in [\![0, k-1]\!]$. Finally, for every $A \subset \underline{\beta}_s$, we define β_A as a parallel copy of $\beta^{|A|}$.

(b) If $\beta \in \underline{\beta}_s$ the construction is similar to the regular case, except that β is replaced by β_- or β_+ depending on whether $\beta \in A$ or not. Note that the marked point m_β splits in two marked points $m_{\beta_+} \in \beta_+$ and $m_{\beta_-} \in \beta_-$.

Figure 12: Definition of β_A: let $\beta \in \underline{\beta}$. For every $A \subset \underline{\beta}_s$ we define β_A as above.

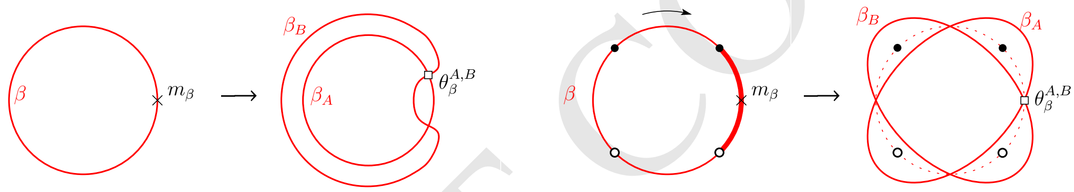

(a) If $\beta \notin B \setminus A$, then β_A and β_B meet twice. We choose $\theta_\beta^{A,B}$ as the point which minimizes the Maslov grading, defined in section 2.3.2, of $\underline{\theta}_A^B$ in $\widehat{\mathrm{CF}}(\underline{\beta}_A, \underline{\beta}_B)$.

(b) If $\beta \in B \setminus A$, then β_A and β_B can be choosen such that they intersect exactly once in each connected component of $\beta \setminus (\underline{z} \cup \underline{w})$. Then we define $\theta_\beta^{A,B}$ as the intersection which lies in the special arc of β, shown in bold.

Figure 13: Definition of $\underline{\theta}_A^B$: let $A \subsetneq B \subset \underline{\beta}_s$. For every $\beta \in \underline{\beta}$, we define $\theta_\beta^{A,B} \in \beta_A \cap \beta_B$ as above and set $\underline{\theta}_A^B := \{\theta_\beta^{A,B}\}_{\beta \in \underline{\beta}}$. By convention and throughout this paper, we represent generator dot elements by black squares and $\underline{\theta}_A^B$ dot elements by white ones.

Finally, we define $\partial_D : \widehat{\mathrm{CF}}(D) \longrightarrow \widehat{\mathrm{CF}}(D)$ as

$$\bigoplus_{A \subset \underline{\beta}_s} \sum_{A \subset B \subset \underline{\beta}_s} f_A^B.$$

2.3.2. *Grading.* We define two relative grading on $\widehat{\mathrm{CF}}(D)$, namely the Maslov grading M and the Alexander grading A, by

$$\begin{aligned} M(\underline{x}) - M(\underline{y}) &= \mu(\phi) - 2n_{\underline{w}}(\phi) + |B \setminus A| \\ A(\underline{x}) - A(\underline{y}) &= n_{\underline{z}}(\phi) - n_{\underline{w}}(\phi) \end{aligned}$$

where A and $B := A \cup \{\beta_1, \cdots, \beta_{|B \setminus A|}\}$ are subsets of $\underline{\beta}_s$, $\underline{x}$ (resp. $\underline{y}$) any generator of $\widehat{\mathrm{CF}}(\underline{\alpha}, \underline{\beta}_A)$ (resp. $\widehat{\mathrm{CF}}(\underline{\alpha}, \underline{\beta}_B)$) and ϕ a Whitney disk in $\pi_2(\underline{x}, \underline{\theta}_A^{A \cup \{\beta_1\}}, \cdots, \underline{\theta}^B_{B \setminus \{\beta_{|B \setminus A|}\}}, \underline{y})$.

Moreover, for every $P \subset \underline{\beta}_s$, we also define a grading S_P which is absolute and defined, for any element $\underline{x} \in \widehat{\mathrm{CF}}(\underline{\alpha}, \underline{\beta}_A)$ where $A \subset \underline{\beta}_s$, by $S(\underline{x}) = |A \cap P|$. For $P = \underline{\beta}_s$, we simply denote it by S and we call it the *singular grading*.

Remark 2.2. For simplicity, we consider in this paper only a single Alexander grading, but it can be straigforwardly extended to a multi-grading by coloring the connected component of the link. Note that it means that two components which share a double point must be colored the same way.

(a) If $\beta \notin B \setminus A$, then $\theta^{A,B}_\beta$ is connected to the second element of $\beta_A \cap \beta_B$ by exactly two disks which cancel one each other.

(b) If $\beta \in B \setminus A$, then all Whitney disks which start at $\theta^{A,B}_\beta$ meet $\underline{w} \cup \underline{z}$.

Figure 14: Proof of Lemma 2.3 for $d = 2$: Let $A \subsetneq B \subset \underline{\beta}_s$. Counting the Whitney disks which meet a given $\beta \in \underline{\beta}$ prove that $f^{\widetilde{\underline{z}},\widetilde{\underline{w}}}_{\underline{\beta}_B,\underline{\beta}_A}(\underline{\theta}^B_A) = 0$.

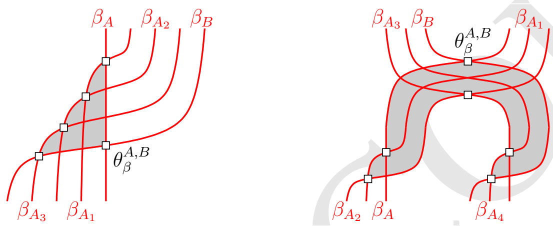

(a) $\beta \notin B \setminus A$

(b) $\beta \in B \setminus A$

Figure 15: Proof of Lemmata 2.4 and 2.3 for $d \geq 3$: Let $A \subsetneq B \subset \underline{\beta}_s$ and $\mathcal{F} \in \mathscr{F}^B_A$ of length $d \geq 3$. Then, among all possibilities, only $\pi_2(A^{\mathcal{F}}, \underline{\theta}^B_A)$ is non empty and it contains a unique element ϕ which splits into maps $\phi_\beta : \mathbb{D} \longrightarrow \Sigma$ for every $\beta \in \underline{\beta}$. They are shown above with shading. The Maslov formula given in [Sar06] shows that $\mu(\phi) = 0$. The image $f^{\underline{z}\cup\underline{w}}_{\boldsymbol{B}^{\mathcal{F}}}(\boldsymbol{\Theta}^{\mathcal{F}})$ is hence null unless $d = 3$. In the latter case, the fact that $\#\mathcal{M}(\phi) = 1$ follows from the Riemann mapping theorem.

2.3.3. *Homology.*

Proposition 2.2. *The couple $(\widehat{\mathrm{CF}}(D), \partial_D)$ is a chain complex which is homologicaly graded by M, by A and filtrated by S.*

Proof. We prove that $(\partial_D)^2 = 0$. To this end, we need the following lemmata whose proofs are given in Fig. 14 and 15.

Lemma 2.3. *For every $A \subset B \subset \underline{\beta}_s$ and every $\mathcal{F} \in \mathscr{F}^B_A$ of length $d \neq 3$,*

$$f^{\underline{z}\cup\underline{w}}_{\boldsymbol{B}^{\mathcal{F}}}(\boldsymbol{\Theta}^{\mathcal{F}}) = 0.$$

Lemma 2.4. *For every $A \subset B \subset \underline{\beta}_s$ and every $\mathcal{F} \in \mathscr{F}^B_A$ of length $d = 3$,*

$$f^{\underline{z}\cup\underline{w}}_{\boldsymbol{B}^{\mathcal{F}}}(\boldsymbol{\Theta}^{\mathcal{F}}) = \underline{\theta}^B_A.$$

Now, we consider a subset $A \subset \underline{\beta}_s$ and an element $\underline{x} \in \widehat{\mathrm{CF}}(\underline{\alpha}, \underline{\beta}_A)$.
Let $\mathcal{F}$ be a flag in $\mathscr{F}^{\subset \underline{\beta}_s}_A$. By applying Th. 2.1 to $(\underline{\alpha}, \boldsymbol{B}^{\mathcal{F}})$ and evaluating it in $\underline{x} \otimes \boldsymbol{\Theta}^{\mathcal{F}}$, we obtain

$$\sum_{1 \leq m \leq d} f^{\underline{z}\cup\underline{w}}_{\underline{\alpha},\boldsymbol{B}^{\mathcal{F}}_{m,d}}\Big(f^{\underline{z}\cup\underline{w}}_{\underline{\alpha},\boldsymbol{B}^{\mathcal{F}}_{1,m}}(\underline{x} \otimes \boldsymbol{\Theta}^{\mathcal{F}}_{1,m}) \otimes \boldsymbol{\Theta}^{\mathcal{F}}_{m,d}\Big)$$

$$= \sum_{1 \leq k \leq d} f^{\underline{z}\cup\underline{w}}_{\underline{\alpha},\boldsymbol{B}^{\mathcal{F}}_{1,k},\boldsymbol{B}^{\mathcal{F}}_{m,d}}\Big(\underline{x} \otimes \boldsymbol{\Theta}^{\mathcal{F}}_{1,k} \otimes f^{\underline{z}\cup\underline{w}}_{\boldsymbol{B}^{\mathcal{F}}_{k,m}}(\boldsymbol{\Theta}^{\mathcal{F}}_{k,m}) \otimes \boldsymbol{\Theta}^{\mathcal{F}}_{m,d}\Big).$$

Since the lemmata, this is equal to

$$(2) \qquad = \sum_{1\leq k\leq d-2} f^{\underline{z}\cup\underline{w}}_{\underline{\alpha},\boldsymbol{B}^{\mathcal{F}}_{1,k},\boldsymbol{B}^{\mathcal{F}}_{k+2,d}}\Big(\underline{\boldsymbol{x}}\otimes\boldsymbol{\Theta}^{\mathcal{F}}_{1,k}\otimes\underline{\boldsymbol{\theta}}^{F_{k+2}}_{F_k}\otimes\boldsymbol{\Theta}^{\mathcal{F}}_{k+2,d}\Big).$$

Now, we sum them for every flag in $\mathscr{F}^{\subset\underline{\boldsymbol{\beta}}_s}_A$. On the left-hand side, we obtain

$$\sum_{\mathcal{F}\in\mathscr{F}^{\subset\underline{\boldsymbol{\beta}}_s}_A}\Bigg(\sum_{1\leq m\leq d} f^{\underline{z}\cup\underline{w}}_{\underline{\alpha},\boldsymbol{B}^{\mathcal{F}}_{m,d}}\Big(f^{\underline{z}\cup\underline{w}}_{\underline{\alpha},\boldsymbol{B}^{\mathcal{F}}_{1,m}}(\underline{\boldsymbol{x}}\otimes\boldsymbol{\Theta}^{\mathcal{F}}_{1,m})\otimes\boldsymbol{\Theta}^{\mathcal{F}}_{m,d}\Big)\Bigg)$$

$$= \sum_{A\subset B\subset C\subset\underline{\boldsymbol{\beta}}_s}\ \sum_{\mathcal{F}^1\in\mathscr{F}^B_A}\ \sum_{\mathcal{F}^2\in\mathscr{F}^C_B} f^{\underline{z}\cup\underline{w}}_{\underline{\alpha},\boldsymbol{B}^{\mathcal{F}^2}}\Big(f^{\underline{z}\cup\underline{w}}_{\underline{\alpha},\boldsymbol{B}^{\mathcal{F}^1}}(\underline{\boldsymbol{x}}\otimes\boldsymbol{\Theta}^{\mathcal{F}^1})\otimes\boldsymbol{\Theta}^{\mathcal{F}^2}\Big).$$

This is equal to

$$\sum_{A\subset B\subset C\subset\underline{\boldsymbol{\beta}}_s}\ \sum_{\mathcal{F}^2\in\mathscr{F}^C_B} f^{\underline{z}\cup\underline{w}}_{\underline{\alpha},\boldsymbol{B}^{\mathcal{F}^2}}\Bigg(\Big(\sum_{\mathcal{F}^1\in\mathscr{F}^B_A} f^{\underline{z}\cup\underline{w}}_{\underline{\alpha},\boldsymbol{B}^{\mathcal{F}^1}}(\underline{\boldsymbol{x}}\otimes\boldsymbol{\Theta}^{\mathcal{F}^1})\Big)\otimes\boldsymbol{\Theta}^{\mathcal{F}^2}\Bigg)$$

$$\begin{aligned} &= \sum_{A\subset B\subset C\subset\underline{\boldsymbol{\beta}}_s} f^C_B\Big(f^B_A(\underline{\boldsymbol{x}})\Big) \\ &= (\partial_D)^2(\underline{\boldsymbol{x}}). \end{aligned}$$

The right-hand side vanishes since all the terms are of the form

$$f^{\underline{z}\cup\underline{w}}_{\underline{\alpha},\boldsymbol{B}^{\mathcal{F}^1},\boldsymbol{B}^{\mathcal{F}^2}}\Big(\underline{\boldsymbol{x}}\otimes\boldsymbol{\Theta}^{\mathcal{F}^1}\otimes\underline{\boldsymbol{\theta}}^{F^2_1}_{F^1_{d^1}}\otimes\boldsymbol{\Theta}^{\mathcal{F}^2}\Big);$$

where $\mathcal{F}^1\in\mathscr{F}^{\subset\underline{\boldsymbol{\beta}}_s}_A$ and $\mathcal{F}^2\in\mathscr{F}^{\subset\underline{\boldsymbol{\beta}}_s}_{F^1_{d^1}\cup\{a,b\}}$ for some distinct $a,b\in\underline{\alpha}_s\setminus F^1_{d^1}$. Indeed, a given such pattern appears as many times as there are flags in $\mathscr{F}^{F^1_{d^1}\cup\{a,b\}}_{F^1_{d_1}}$, and there are exactly two such flags.

This is true for every $A\subset\underline{\boldsymbol{\beta}}_s$ and every $\underline{\boldsymbol{x}}\in\widehat{\mathrm{CF}}(\underline{\alpha},\underline{\boldsymbol{\beta}}_A)$, hence $\partial^2_D(\underline{\boldsymbol{x}})=0$ for every $\underline{\boldsymbol{x}}\in\widehat{\mathrm{CF}}(D)$.
The affirmation on grading and filtration is clearly satisfied. □

Definition 2.1. A leveled module (H,k) is a module H together with a level $k\in\mathbb{Z}$.
A tensor product of graded modules is naturally graded by the sum of the summand grading.
We say that two leveled bigraded modules (H_1,k_1) and (H_2,k_2) with $k_1\leq k_2$ are stable equivalent if $H_2\cong H_1\otimes A^{\otimes(k_2-k_1)}$ where A is a module freely generated by two elements whose bigrading differ by $(1,1)$.

Theorem 2.5. *The stable class of $\Big(H_*(\widehat{\mathrm{CF}}(D),\partial_D),\#\underline{z}-1\Big)$, denoted by $\lfloor\widehat{\mathrm{HFV}}(L,Y)\rfloor$, depends only on the underlying singular oriented link L and on the orientations of its double points.*

The section 3.3 is devoted to the proof of this theorem.

According to Prop. 1.1, there exists a diagram for L such that $\#\underline{z}=\ell_r+2s$ where s is the number of double points in L and ℓ_r is the number of regular component (*i.e.* with no double point). There is hence a bigraded module leveled by ℓ_r+2s-1 in $\lfloor\widehat{\mathrm{HFV}}(L,Y)\rfloor$. We denote by $\widetilde{\mathrm{HFV}}(L,Y)$ this module.

We will prove latter that there even exists a bigraded module leveled by $\ell-1$, where ℓ is the total number of components in L, in $\lfloor\widehat{\mathrm{HFV}}(L,Y)\rfloor$. We denote by $\widehat{\mathrm{HFV}}(L,Y)$ this module.

3. Properties of $\widehat{\mathrm{HFV}}$

In this section, we keep the notation from section 2.3.

3.1. **Exact triangle.** In this section, we prove that the three link Floer homologies of a singular link and of the two desingularizations of one of its double points fit an exact triangle.

Proposition 3.1. *For any double point p of L, $\widehat{\mathrm{CF}}(D)$ can be seen as the mapping cone of a morphism $f_p\colon \widehat{\mathrm{CF}}(D_+) \longrightarrow \widehat{\mathrm{CF}}(D_-)$ where D_+ and D_- correspond, respectively, to the positive and the negative resolutions of the arc $\beta_p \in \underline{\boldsymbol{\beta}}_s$ associated to p.*

Proof. By construction, we have

$$\widehat{\mathrm{CF}}(D_+) = \bigoplus_{\substack{A\subset\underline{\boldsymbol{\beta}}_s\\ \beta_p\notin A}} \widehat{\mathrm{CF}}(\underline{\boldsymbol{\alpha}},\underline{\boldsymbol{\beta}}_A), \qquad \text{and} \qquad \widehat{\mathrm{CF}}(D_-) = \bigoplus_{\substack{A\subset\underline{\boldsymbol{\beta}}_s\\ \beta_p\in A}} \widehat{\mathrm{CF}}(\underline{\boldsymbol{\alpha}},\underline{\boldsymbol{\beta}}_A).$$

Then $\widehat{\mathrm{CF}}(D)$ can be seen as $\widehat{\mathrm{CF}}(D_+)\oplus\widehat{\mathrm{CF}}(D_-)$. We denote by ∂_+ (resp. ∂_-) the restriction of ∂_D on $\widehat{\mathrm{CF}}(D_+)$ (resp. $\widehat{\mathrm{CF}}(D_-)$) composed with the projection on $\widehat{\mathrm{CF}}(D_+)$ (resp. $\widehat{\mathrm{CF}}(D_-)$). Now, we define $f_p\colon \widehat{\mathrm{CF}}(D_+) \longrightarrow \widehat{\mathrm{CF}}(D_-)$ by

$$f_p(\underline{\boldsymbol{x}}) := \bigoplus_{\substack{A\subset\underline{\boldsymbol{\beta}}_s\\ \beta_p\notin A}} \sum_{\substack{A\subset B\subset\underline{\boldsymbol{\beta}}_s\\ \beta_p\in B}} \sum_{\mathcal{F}\in\mathscr{F}_A^B} f^{\underline{\boldsymbol{z}}\cup\underline{\boldsymbol{w}}}_{\underline{\boldsymbol{\alpha}},\underline{\boldsymbol{B}}^{\mathcal{F}}}(\underline{\boldsymbol{x}}\otimes\boldsymbol{\Theta}^{\mathcal{F}})$$

for every $\underline{\boldsymbol{x}} \in \widehat{\mathrm{CF}}(D_+)$. It is is a chain morphism since

$$f_p\circ\partial_{D_+} + \partial_{D_-}\circ f_p = (\partial_+)^2 + f_p\circ\partial_+ + \partial_-\circ f_p + (\partial_-)^2 = (\partial_D)^2 = 0.$$

It is immediate to check that $\mathrm{Cone}(f_p)\cong\widehat{\mathrm{CF}}(D)$. □

Corollary 3.2. *For any double point p of L and at each level greater than $\ell_r + 2s - 1$, there is an exact triangle*

$$\begin{tikzcd} \lfloor\widehat{\mathrm{HFV}}(L_+)\rfloor \arrow[rr] & & \lfloor\widehat{\mathrm{HFV}}(L_-)\rfloor \arrow[dl] \\ & \lfloor\widehat{\mathrm{HFV}}(L)\rfloor \arrow[ul] & \end{tikzcd}$$

where L_+ and L_- are, respectively, the positive and the negative resolutions of p.

Corollary 3.3. *For every subset $P \in \underline{\boldsymbol{\beta}}_s$, the map ∂_D respects the filtration associated to the grading S_P. The homology of the associated graded part is, up to some shifting in the grading M and A, the direct sum of the link Floer homologies of all the link obtained by desingularizing the double points of L associated to the elements of P.*

This corollary is very helpful for reducing isomorphism proofs to the regular case.

3.2. **Singular connected sum.** Let $L_1 \subset Y_1$ and $L_2 \subset Y_2$ be two oriented links, possibly singular, and let o_1, o_2 be orientations for their double points. Now let $m_1 \in L_1$ and $m_2 \in L_2$ be two distinguished regular points. By $L_1\,{}_{m_1}\#_{m_2}\,L_2$ we denote the connected sum of L_1 and L_2 near m_1 and m_2 in $Y_1\#Y_2$ and by $L_1\,{}_{m_1}\#^s_{m_2}\,L_2$ their singular connected sum which is a singularization of $L_1\,{}_{m_1}\#_{m_2}\,L_2$ located at their fuzioning points. In this section, we prove that the link Floer homologies of all these links are related in a simple way.

For $i \in \{1,2\}$, let $D_i = (\Sigma_i, \underline{\boldsymbol{\alpha}}_i, \underline{\boldsymbol{\beta}}_i, \underline{\boldsymbol{z}}_i, \underline{\boldsymbol{w}}_i)$ be a Heegaard diagram for L_i such that $z^* \in \underline{\boldsymbol{z}}_1$ represents $m_1 \in L_1$ and $w^* \in \underline{\boldsymbol{w}}_2$ represents $m_2 \in L_2$. Then, as shown in Fig. 16,

$$D_\# = \Big(\Sigma_1\#\Sigma_2, \underline{\boldsymbol{\alpha}}_1 \cup \underline{\boldsymbol{\alpha}}_2, \underline{\boldsymbol{\beta}}_1 \cup \underline{\boldsymbol{\beta}}_2, (\underline{\boldsymbol{z}}_1 \cup \underline{\boldsymbol{z}}_2)\setminus\{z^*\}, (\underline{\boldsymbol{w}}_1 \cup \underline{\boldsymbol{w}}_2)\setminus\{w^*\}\Big)$$

is a diagram for $L_1\,{}_{m_1}\#_{m_2}\,L_2$.

Definition 3.1. Let (C_1,∂_1) and (C_2,∂_2) be two chain complexes repectively endowed with $\mathbb{Z}$–grading gr_1 and gr_2. Then $C_1\otimes C_2$ is naturally endowed with a differential ∂ defined for every elements $x_1 \in C_1$ and $x_2 \in C_2$ by $\partial(x\otimes y) = \partial_1(x)\otimes y + x\otimes\partial_2(y)$.

Proposition 3.4. *With the notation above, the chain complexes $\widehat{\mathrm{CF}}(D_\#)$ and $\widehat{\mathrm{CF}}(D_1)\otimes\widehat{\mathrm{CF}}(D_2)$ are isomorphic.*

On the basis of remark 3.1, the proof is a straightforward adaptation of the proof of Th. 11.1 in [OS08] where the chain map defined by counting pseudo-holomorphic triangles is replaced by a chain map which counts pseudo-holomorphic polygons.

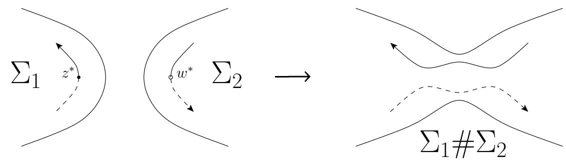

Figure 16: Heegaard diagrams for connected sums

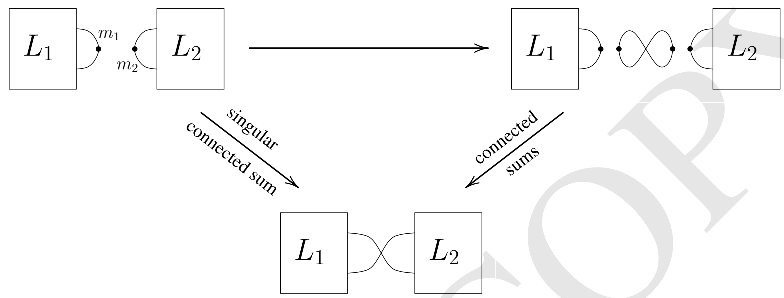

Figure 17: Singular connected sums seen as regular ones

Definition 3.2. A tensor product of leveled modules is naturally leveled by the sum of the two summands levels.

Proposition 3.5. *With the notation above,*

$$\lfloor\widehat{\mathrm{HFV}}(L_{1\ m_1}\#_{m_2}\,L_2, Y_1\#Y_2)\rfloor \cong \lfloor\widehat{\mathrm{HFV}}(L_1, Y_1)\rfloor \otimes \lfloor\widehat{\mathrm{HFV}}(L_2, Y_2)\rfloor.$$

Proof. It follows from standard algebra and the fact that $\#((\underline{z}_1 \cup \underline{z}_2) \setminus \{z^*\}) - 1 = (\#\underline{z}_1 - 1) + (\#\underline{z}_2 - 1)$. □

Likewise, by considering a once pointed diagram of the linkfree space, one can prove a similar statement on the embedding of a link inside a connected sum of spaces.

Proposition 3.6. *With the notation above,*

$$\lfloor\widehat{\mathrm{HFV}}(L_1, Y_1\#Y_2)\rfloor \cong \lfloor\widehat{\mathrm{HFV}}(L_1, Y_1)\rfloor \otimes (\widehat{\mathrm{HF}}Y_2, 0)$$

where $\widehat{\mathrm{HF}}(Y_2)$ *is endowed with trivial Alexander grading and singular filtration.*

Proposition 3.7. *With same notation,* $\widehat{\mathrm{HFV}}(L_{1\ m_1}\#^{s}_{m_2}\,L_2, Y_1\#Y_2) \equiv 0$.

Proof. As shown in Fig. 17, any singular connected sum can be replaced by two regular ones on the once-singularized unknot K_∞. According to Prop. 3.5, it is sufficient to prove that $\widehat{\mathrm{HF}}(K_\infty) \equiv 0$.

A singular Heegaard diagram for K_∞ is given in Fig. 18. Note that, because of the symmetry (on the sphere), the choice of orientation for the double point is of no importance. It is easily seen that the associated chain complex has four generators, denoted in Fig. 18 by 1, 2, 3 and 4 and that the differential involves only two Whitney triangles. This gives $\partial(1) = 4$, $\partial(3) = 2$ and the resulting homology is null.

□

3.3. **Invariance.** To prove Th. 2.5, we need to check the invariance under the following operations:

i. changing the pseudo-holomorphic structure on Σ;
ii. arc isotopies;
iii. regular and singular handleslides;

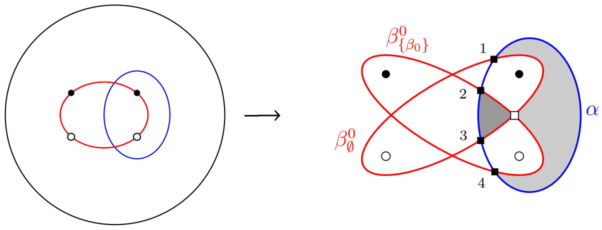

Figure 18: A diagram on S^2 for K_∞: the two Whitney triangles are shown on the right with different shading.

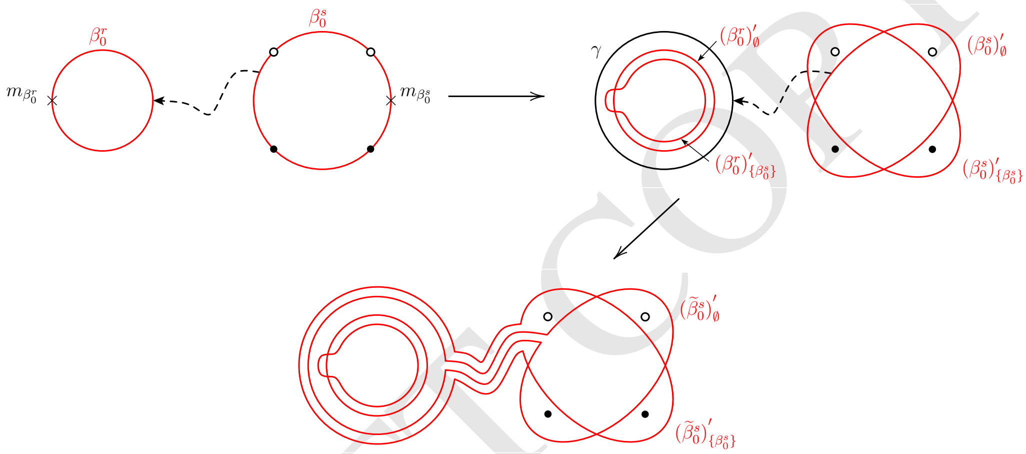

Figure 19: Definition of β'_A for a singular handleslide

iv. index zero/three (de)stabilizations;
v. index one/two (de)stabilizations;
vi. moving a point m_β;
vii. moving an element of $\beta_+ \cap \beta_-$.

An arc isotopie can be seen as a special case of the first operation. The proof of invariance under the operations *i.*, *iii.*, *vi.* and *vii.* are similar, so we only treat in details the case of singular handleslides.

3.3.1. *Singular handleslides.* Let $D' = (\Sigma, \underline{\alpha}, \underline{\beta}', \underline{z}, \underline{w})$ be a Heegaard diagram obtained from D by performing a singular $\boldsymbol{\beta}$–handleslide of $\beta_0^s \in \underline{\beta}_s$ over $\beta_0^r \in \underline{\beta}_r$.

Let $\beta \in \underline{\beta}$. For every $A \subset \underline{\beta}_s \simeq \underline{\beta}'_s$, we define β'_A using the algorithm of Fig. 12 but performed on $\beta_{\underline{\beta}_s}$ instead of β. Equivalently, we define together $\{\beta_A\}_{A\subset\underline{\beta}_s} \cup \{\beta'_A\}_{A\subset\underline{\beta}'_s}$ as in Fig. 12 but with $|A|$ replaced by $(|A| + |\underline{\beta}_s| + 1)$ for every $A \subset \underline{\beta}'_s$. Then we consider γ, a parallel copy of β_0^r which does not meet $(\beta_0^r)_A$ for any $A \subset \underline{\beta}_s$, but which meet the handleslide arc from β_0^s to β_0^r. Now, we define successively the $(\widetilde{\beta_0^s})'_A$ for all $A \subset \underline{\beta}_s$ as handleslides of the $(\beta_0^s)'_A$ over γ (see Fig. 19). Finally, for every $A \subset \underline{\beta}_s$, we set $\underline{\beta}'_A := \left(\{\beta'_A\}_{\beta\in\underline{\beta}} \setminus \{(\beta_0^s)'_A\}\right) \cup \{(\widetilde{\beta_0^s})'_A\}$.

One can check that the set $\{\underline{\beta}'_A | A \subset \underline{\beta}_s\}$ is admissible for the construction given in section 2.3.

Now, we denote by $\underline{\theta}_A$ the intersection point in $\mathbb{T}_{\underline{\beta}_A} \cap \mathbb{T}_{\underline{\beta}'_A}$ which maximizes the Maslov grading in $\widehat{\mathrm{CF}}(\underline{\beta}_A, \underline{\beta}'_A)$. Then, using the notation from section 2.3 but adding a subscript to indicate the diagram we are

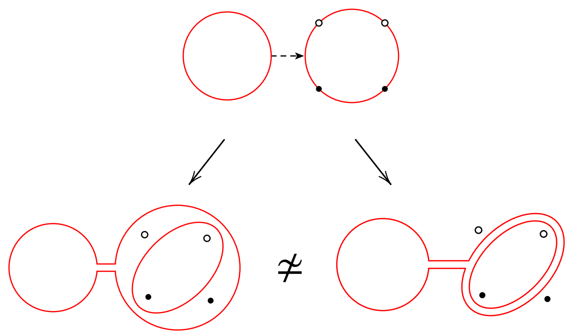

Figure 20: Obstruction for invariance under non authorized singular handleslide

dealing with, we set for every $A \subset C \subset \underline{\boldsymbol{\beta}}_s$ the map $f^{\mathrm{sh}}_{A,C} \colon \widehat{\mathrm{CF}}(\underline{\boldsymbol{\alpha}}, \underline{\boldsymbol{\beta}}_A) \longrightarrow \widehat{\mathrm{CF}}(\underline{\boldsymbol{\alpha}}, \underline{\boldsymbol{\beta}}'_C)$ by

$$f^{\mathrm{sh}}_{A,C}(\underline{\boldsymbol{x}}) := \sum_{A \subset B \subset C} \sum_{\substack{\mathcal{F}^1 \in \mathscr{F}^B_A \\ \mathcal{F}^2 \in \mathscr{F}^C_B}} f^{\underline{z} \cup \underline{\boldsymbol{w}}}_{\underline{\boldsymbol{\alpha}}, \boldsymbol{B}^{\mathcal{F}^1}_D, \boldsymbol{B}^{\mathcal{F}^2}_{D'}}(\underline{\boldsymbol{x}} \otimes \boldsymbol{\Theta}^{\mathcal{F}^1}_D \otimes \underline{\boldsymbol{\theta}}_B \otimes \boldsymbol{\Theta}^{\mathcal{F}^2}_{D'})$$

for every $\underline{\boldsymbol{x}} \in \mathrm{CF}^-(\underline{\boldsymbol{\alpha}}, \underline{\boldsymbol{\beta}}_A)$. Finally, we define $f^{\mathrm{sh}} \colon \widehat{\mathrm{CF}}(D) \longrightarrow \widehat{\mathrm{CF}}(D')$ as

$$\bigoplus_{A \subset \underline{\boldsymbol{\beta}}_s} \sum_{A \subset C \subset \underline{\boldsymbol{\beta}}_s} f^{\mathrm{sh}}_{A,C}.$$

By an argument similar to the proof of Prop. 2.2, one can prove that $f^{\mathrm{sh}} \circ \partial_D + \partial_{D'} \circ f^{\mathrm{sh}} = 0$. It is hence a chain map which clearly respects the singular filtration. Moreover, the associated graded part is the direct sum, for every $A \subset \underline{\boldsymbol{\beta}}_s$, of the maps

$$f^{\mathrm{sh}}_A \colon \begin{array}{ccc} \widehat{\mathrm{CF}}(\underline{\boldsymbol{\alpha}}, \underline{\boldsymbol{\beta}}_A) & \longrightarrow & \widehat{\mathrm{CF}}(\underline{\boldsymbol{\alpha}}, \underline{\boldsymbol{\beta}}'_A) \\ \underline{\boldsymbol{x}} & \longmapsto & f^{\underline{z} \cup \underline{\boldsymbol{w}}}_{\underline{\boldsymbol{\alpha}}, \underline{\boldsymbol{\beta}}_A, \underline{\boldsymbol{\beta}}'_A}(\underline{\boldsymbol{x}} \otimes \underline{\boldsymbol{\theta}}_A) \end{array},$$

which are the invariance maps for $\boldsymbol{\beta}$–handleslide in the regular case. For instance in [Sah10], they are proven to be quasi–isomorphisms. The whole map f^{sh} is hence an quasi–isomorphism.

Remark 3.1. The same outlines — *i.e.* using the technics developped in section 2.3 to define a chain map $f \colon \widehat{\mathrm{CF}}(D) \longrightarrow \widehat{\mathrm{CF}}(D')$ which respects the singular filtration and then proving that the graded part is an isomorphism since it corresponds to an invariance map from the regular world — can be adapted to the other cases. However, it is not working for an handleslide of a regular circle β^r_0 over a singular one β^s_0, since the set $\underline{\boldsymbol{\beta}}'_A$ defined above for any given $A \subset \underline{\boldsymbol{\beta}}_s$ does not correspond to an handleslide of $(\beta^r_0)_A$ over $(\beta^s_0)_A$ (see Fig. 20).

3.3.2. *Index zero/three and regular one/two (de)stabilizations.* Index one/two stabilizations can be seen as a connected sums with an empty copy of S^3. But since $\widehat{\mathrm{HF}}(S^3) \cong \mathbb{F}_2$, Prop. 3.6 achieve the proof. The argument is valid only when attaching the new handle to a pointed domain. However, it can be then moved among domains *via* handleslides.

Regular index zero/three stabilizations can also be seen as a connected sum with the trivial link in S^3. Since $\lfloor \widehat{\mathrm{HFV}}(\mathrm{Unknot}, S^3) \rfloor \cong \lfloor (\mathbb{F}_2, 0) \rfloor$, Prop. 3.5 concludes the proof.

3.3.3. *Singular one/two (de)stabilizations.* Let $D' := (\Sigma, \underline{\alpha}', \underline{\beta}', \underline{z}', \underline{w}')$ be a Heegaard diagram obtained from D by performing an index one/two stabilization on a element $z^* \in \underline{z} \cap \beta^*$ for a given $\beta^* \in \underline{\boldsymbol{\beta}}_s$. We denote by α', β', z' and w' the new elements. We also denote by p^* the singular point of L corresponding to β^* and by $bbeta^*_s$ the set $bbeta_s \setminus \{\beta^*\}$.

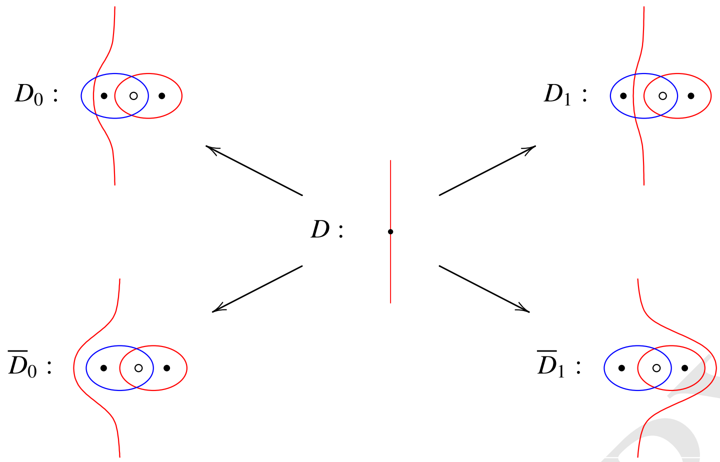

Figure 21: Perturbations of D: in a neighborhood of z^*, the four diagrams are depicted above. Outside they are all small perturbations of D such that, on every connected component, any two perturbations meet exactly twice and transversaly.

Now, let D_0, D_1, $\overline{D}_0$ and $\overline{D}_1$ be the four diagrams depicted in Fig. 21. In particular, D_0 and $\overline{D}_0$ are diagrams for the positive desingularization of p^* whereas D_1 and $\overline{D}_1$ are diagrams for the negative one. Moreover, under the terms of Prop. 3.1, we have $\widehat{\mathrm{CF}}(D') \cong \mathrm{Cone}(f_{p^*} : \widehat{\mathrm{CF}}(D_0) \longrightarrow \widehat{\mathrm{CF}}(D_1))$. Exactly in the same way as f_{p^*}, we can define a map $\overline{f}_{p^*} : \widehat{\mathrm{CF}}(\overline{D}_0) \longrightarrow \widehat{\mathrm{CF}}(\overline{D}_1)$.

Now, we want to prove, as a first step, that $\mathrm{Cone}(f_{p^*})$ and $\mathrm{Cone}(\overline{f}_{p^*})$ are quasi-isomorphic. Since the diagrams differ by isotopies and handleslides, we already have quasi-isomorphisms $f_0 \colon \widehat{\mathrm{CF}}(D_0) \longrightarrow \widehat{\mathrm{CF}}(\overline{D}_0)$ and $f_1 \colon \widehat{\mathrm{CF}}(D_1) \longrightarrow \widehat{\mathrm{CF}}(\overline{D}_1)$. For every $A \subset \underline{\boldsymbol{\beta}}^*_s$ and for $f \colon \widehat{\mathrm{CF}}(\underline{\boldsymbol{\alpha}}, \underline{\boldsymbol{\beta}}_0) \longrightarrow \widehat{\mathrm{CF}}(\underline{\boldsymbol{\alpha}}, \underline{\boldsymbol{\beta}}_1) \in \{f_{p^*}, \overline{f}_{p^*}, f_0, f_1\}$, let's θ^f_A be the top-dimensional element of $\widehat{\mathrm{CF}}(\underline{\boldsymbol{\beta}}_0, \underline{\boldsymbol{\beta}}_1)$ used to define f. We define two maps $g_0, g_1 \colon \widehat{\mathrm{CF}}(D_0) \longrightarrow \widehat{\mathrm{CF}}(\overline{D}_1)$ as, respectively,

$$\bigoplus_{A\subset\underline{\boldsymbol{\beta}}^*_s} \sum_{A\subset B\subset C\subset D\subset\underline{\boldsymbol{\beta}}^*_s} \sum_{\substack{\mathcal{F}^1\in\mathscr{F}^B_A\\ \mathcal{F}^2\in\mathscr{F}^C_B\\ \mathcal{F}^3\in\mathscr{F}^D_C}} f^{\underline{\boldsymbol{z}}\cup\underline{\boldsymbol{w}}}_{\underline{\boldsymbol{\alpha}},\boldsymbol{B}^{\mathcal{F}^1}_{D_0},\boldsymbol{B}^{\mathcal{F}^2}_{\overline{D}_0},\boldsymbol{B}^{\mathcal{F}^3}_{\overline{D}_1}}\big(\,.\,\otimes\boldsymbol{\Theta}^{\mathcal{F}^1}_{D_0}\otimes\underline{\boldsymbol{\theta}}^{f_0}_B\otimes\boldsymbol{\Theta}^{\mathcal{F}^2}_{\overline{D}_0}\otimes\underline{\boldsymbol{\theta}}^{\overline{f}_0}_C\otimes\boldsymbol{\Theta}^{\mathcal{F}^3}_{\overline{D}_1}\big)$$

and

$$\bigoplus_{A\subset\underline{\boldsymbol{\beta}}^*_s} \sum_{A\subset B\subset C\subset D\subset\underline{\boldsymbol{\beta}}^*_s} \sum_{\substack{\mathcal{F}^1\in\mathscr{F}^B_A\\ \mathcal{F}^2\in\mathscr{F}^C_B\\ \mathcal{F}^3\in\mathscr{F}^D_C}} f^{\underline{\boldsymbol{z}}\cup\underline{\boldsymbol{w}}}_{\underline{\boldsymbol{\alpha}},\boldsymbol{B}^{\mathcal{F}^1}_{D_0},\boldsymbol{B}^{\mathcal{F}^2}_{D_1},\boldsymbol{B}^{\mathcal{F}^3}_{\overline{D}_1}}\big(\,.\,\otimes\boldsymbol{\Theta}^{\mathcal{F}^1}_{D_0}\otimes\underline{\boldsymbol{\theta}}^{f_{p^*}}_B\otimes\boldsymbol{\Theta}^{\mathcal{F}^2}_{D_1}\otimes\underline{\boldsymbol{\theta}}^{f_1}_C\otimes\boldsymbol{\Theta}^{\mathcal{F}^3}_{\overline{D}_1}\big)$$

where the subscript on $\boldsymbol{B}$ and $\boldsymbol{\Theta}$ symbols indicate the diagram we are dealing with. We obtain the following diagram:

$$\begin{tikzcd}
\widehat{\mathrm{CF}}(D_0) \arrow[loop left, "\partial_{D_0}"] \arrow[r, "f_{p^*}"] \arrow[d, "f_0"'] \arrow[dr, shift left, "g_1"] \arrow[dr, shift right, "g_0"'] & \widehat{\mathrm{CF}}(D_1) \arrow[loop right, "\partial_{D_1}"] \arrow[d, "f_1"] \\
\widehat{\mathrm{CF}}(\overline{D}_0) \arrow[loop left, "\partial_{\overline{D}_0}"] \arrow[r, "\overline{f}_{p^*}"'] & \widehat{\mathrm{CF}}(\overline{D}_1) \arrow[loop right, "\partial_{\overline{D}_1}"]
\end{tikzcd}.$$

As in the proof of Prop. 2.2, it follows from Th. 2.1 that $g_0 \circ \partial_{D_0} + \overline{f}_{p^*} \circ f_0 + \partial_{\overline{D}_1} \circ g_0 = 0$ and $g_1 \circ \partial_{D_0} + f_1 \circ f_{p^*} + \partial_{\overline{D}_1} \circ g_1 = 0$. These formulae prove that the linear map $f^{st} \colon \widehat{\mathrm{CF}}(D_0) \oplus \widehat{\mathrm{CF}}(D_1) \longrightarrow \widehat{\mathrm{CF}}(\overline{D}_0) \oplus \widehat{\mathrm{CF}}(\overline{D}_1)$ defined as

$$\begin{pmatrix} f_0 & 0 \\ g_0 + g_1 & f_1 \end{pmatrix}$$

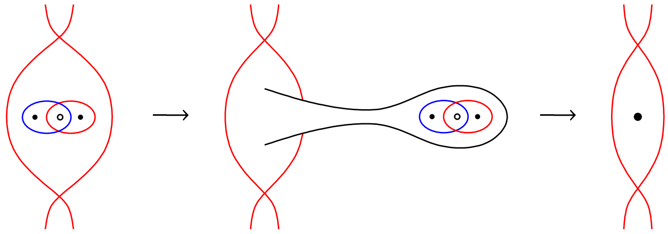

Figure 22: Substituing (sufficiently long) neck for dot

is a chain map between $\mathrm{Cone}(f_{p^*})$ and $\mathrm{Cone}(\overline{f}_{p^*})$ and since its graded part associated to the filtration $S_{\{\beta^*\}}$ is a sum of quasi-isomorphism, the whole map f^{st} is a quasi-isomorphism.

Now, the standard "long neck" argument can be applied to $\mathrm{Cone}(f_{p^*})$. Indeed, α' and β' in $\overline{D}_0$ and $\overline{D}_1$ can be seen as the result of a connected sum with a 2–sphere along a neck. If it is sufficiently long, the neck cannot be involved in any Whitney disk counted by $\partial_{\overline{D}_0}$, $\overline{f}_{p^*}$ nor $\partial_{\overline{D}_1}$ otherwise Gromov compacity would produce a positive periodic domain which does not intersect $\underline{z}$ nor $\underline{w}$. This has two consequences:

- $\mathrm{Cone}(f_{p^*})$ splits in two summands C_1 and C_2, one for each element in $\alpha' \cup \beta'$;
- the neck and the 2–sphere acts just like a dot that Whitney disks cannot intersect. Doing such a substitution is equivalent to coming back to D (see Fig. 22).

The complexes C_1 and C_2 are then both isomorphic to $\widehat{\mathrm{CF}}(D)$ and since corresponding generators in C_1 and C_2 are connected by a bigon ϕ with $\#(\phi \cap \underline{w}) = 1$ and $\#(\phi \cap \underline{z}) = 0$, it follows that $\widehat{\mathrm{CF}}(D')$ is quasi-isomorphic to $\widehat{\mathrm{CF}}(D) \otimes A$.

4. Conjectures

Singular link Floer homology was first motivated by the hope of finite type properties, whatever this may mean, of knot Floer homology.

Thanks to the combinatorial description, many computations have been made and they led to some conjectures.

Conjecture 1. *For every singular link $L \subset Y$ with k double points, there exists an orientation o for the double points such that $\widehat{\mathrm{HFV}}(L, o, Y)$ factorizes by $V^{\otimes k}$.*

Besides being a direct categorification of the finite type properties of the Alexander polynomial, this conjecture have the following consequences:

Corollary 4.1. *If $P(t, q)$ is the Poincaré polynomial of the regular knot Floer homology, then, for every $n \in \mathbb{N}^*$, the image of $P(1, q)$ in $\mathbb{Z}[q]/(2, (1+q)^n)$ is an invariant of finite type.*

Corollary 4.2. *Invariants of finite type with $\mathbb{Z}/2\mathbb{Z}$ coefficients detect the Seifert genus of fibered knots.*

Proof. The width in Alexander grading of the Poincaré polynomial of knot Floer homology is known to be equal to $2g$ where g is the Seifert genus. Moreover, since the extremal coefficient for fibered knots are equal to 1, it remains true for the reduction modulo 2. □

Corollary 4.3. *Among fibered knots, invariants of finite type with $\mathbb{Z}/2\mathbb{Z}$ coefficients detect the unknot.*

For knots in S^3, we have a more precise conjecture:

Conjecture 2. *Let $K \subset S^3$ be a knot which admits a presentation as a composition of a regular tangles T_r, i.e. a tangle with no double point and a purely singular one T_s, i.e. a tangle with only singular crossing and such that among the four strands leaving a given double point, at least two are not attached to the border of T_s (see e.g. Fig. 23). Then, the orientation of the double points of K induced by the orientation of the plane on which T_s is drawn is a suitable choice for applying conjecture 1.*

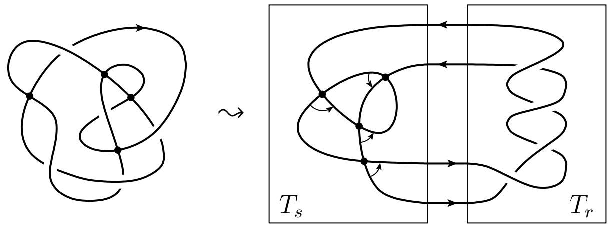

Figure 23: An example of composition between a regular tangle and a purely singular one

Corollary 4.4. *If $K \subset S^3$ is a purely singular knot, i.e. a knot which admits a planar diagram whose crossing are all singular, and if its double points are given the orientation o which corresponds to the orientation of the plane where such a diagram is drawn on, then its link Floer homology vanishes.*

Proof. Let D be a planar diagram for K with $k \in \mathbb{N}^*$ singular crossing and no regular one. Then, Seifert algorithm give a Seifert surface for any desingularization of K with Euler charateristic $d - k$ where $d \in \mathbb{N}^*$ is the number of connected component of the Seifert smoothing of D. It corresponds to a genus of $\frac{1+k-d}{2}$ and the width in Alexander grading of the link Floer homology of any desingularization of K is hence bounded above by $1+k-d \leq k$. But according to Conjecture 2, $\widehat{\mathrm{HFV}}(L, o, S^3)$ has a $\mathcal{H}^{\otimes k}$ factor which is of Alexander width $k + 1$. The homology $\widehat{\mathrm{HFV}}(L, o, S^3)$ is hence null. □

References

[Aud10] Benjamin Audoux, *Singular link floer homology*, Alg. Geom. Top. **9** (2010), 1–35.
[OS04a] Peter Ozsváth and Zoltán Szabó, *Holomorphic disks and knot invariants*, Adv. Math. **186** (2004), no. 1, 58–116.
[OS04b] ———, *Holomorphic disks and three-manifold invariants: properties and applications*, Ann. of Math. (2) **159** (2004), no. 3, 1159–1245.
[OS04c] ———, *Holomorphic disks and topological invariants for closed three-manifolds*, Ann. of Math. (2) **159** (2004), no. 3, 1027–1158.
[OS05] ———, *On the heegaard floer homology of branched double-covers*, Adv. Math. **194** (2005), no. 1, 1–33.
[OS06a] ———, *Holomorphic triangles and invariants for smooth four-manifolds*, Adv. Math. **202** (2006), no. 2, 326–400.
[OS06b] ———, *Introduction to Heegaard Floer theory*, Clay Math. Proc. **5** (2006), 3–28.
[OS06c] ———, *Lectures on Heegaard Floer homology*, Clay Math. Proc. **5** (2006), 29–70.
[OS08] ———, *Holomorphic disks, link invariants and the multi-variable Alexander polynomial*, Algebr. Geom. Topol. **8** (2008), no. 2, 615–692.
[Ras03] Jacob Rasmussen, *Floer homology and knot complements*, Ph.D. thesis, Harvard University, 2003.
[Sah10] Bijan Sahamie, *Introduction to the basics of Heegaard Floer homology*, arXiv:1003.6041, 2010.
[Sar06] Sucharit Sarkar, *Maslov index formulas for Whitney n–gons*, arXiv:math/0609673, 2006.

CMI, Université de Provence, 39 rue Frédéric Joliot-Curie 13453 Marseille cedex 13, France
E-mail address: audoux@cmi.univ-mrs.fr